Four-Switch Buck-Boost Converter Based on Model Predictive Control with Smooth Mode Transition Capability

Xiao Li, *Member, IEEE*, Yushan Liu, *Senior Member, IEEE*, Yaosuo Xue, *Senior Member, IEEE*

***Abstract*— Four-switch buck-boost converter supports both voltage step-up and step-down functionalities, but it suffers from mode transfer challenge that would need reliable mode detection when designed to operate in multi different modes. In this paper, a novel control method based on model predictive current control is proposed for such converter with inherent smooth mode transfer capability without extra design on mode detection and transfer scheme. Modulator and mode detection are replaced by an optimization process through cost function. This largely simplifies the design and makes it easily implemented. Seamless transfer between buck and boost modes is achieved with many other system level benefits. Simulation and experimental results are provided to verify the effectiveness of proposed method for the four-switch buck-boost converter.**

***Index Terms*— Buck-boost converter; model predictive control; seamless transfer; voltage regulation.**

I. INTRODUCTION

The four-switch buck-boost converter, as a non-inverting buck-boost converter, has advantages of wide operating voltage range and capability to step up and down the input voltage [1]-[4]. It also allows bidirectional power flow, which makes this kind of converter suitable for many applications, such as battery power application, solar generating system, and consumer electronics with universal serial bus power delivery (USB PD) design. Fundamentally, there are two basic operating modes, buck mode and boost mode. By pulsating the two separate phases and working equivalently in either buck or boost condition, the converter can implement either step down or step up function per operating condition requirement.

Many existing controllers of the four-switch buck-boost converter were implemented by allowing multi-mode operation [4]. However, the system suffers from mode transfer issues [6]-[8]. Normally, both buck converter and boost converter cannot work in 1:1 voltage ratio condition in high power case with N-FET due to min/max limitation on duty cycle and the non-ideality of parameters existing in power stage [5]. This results in unexpected deadzone, which could come with bad output transient especially when circuit goes through the region where input voltage is very closed to output voltage. The four-switch buck-boost converter system inherits the mode transfer issues with large current and output voltage ripple [6]-[8].

In order to overcome that, some controllers introduce extra operating modes [4], [9], [10], such as buck-boost working mode, which only kicks in when circuit goes through mode transition working regions. These kinds of methods were proved with capability to reduce the deadzone, but at the same time, it will also introduce many other issues, such as low efficiency during buck-boost operation and complex control structure with more design efforts needed. In general, it suffers from the issue of design complexity and the fact that they all rely on accurate and fast mode detection. It also needs designer to design separate compensation stage for buck and boost mode in order to achieve preferred loop performance of each, since buck and boost exhibit different transfer functions and different input/output impedance characteristics [11]-[13]. Right-half plain zero existing in both boost and buck-boost transfer functions would limit the loop optimization and make it hard to share the same loop for different modes [14]. Moreover, a separate modulator for each mode is normally needed in order to get optimized system performance. Thus, it is time consuming to do the loop design for such converter, which relies on engineer's experience a lot. Another extra requirement is the design on mode detection [15]-[17], which is normally conducted through either duty cycle or direct voltage detection. This depends on accurate and reliable synchronization and it could be easily coupled with loop transient. It is far more difficult than thoughts to achieve reliable mode detection with fast response due to the tradeoff between noise immunity and transient. Most existing controllers only do analysis and design for continuous conduction mode (CCM) without providing a solution for discontinuous conduction mode (DCM) [15]-[21], which is normally preferred to improve the light-load efficiency. Also, the discontinuous inductor current charging output capacitor would cause another design challenge for designers [11]-[14].

In order to overcome all issues mentioned above, a new controller for four-switch buck-boost converter is proposed in this paper using model predictive control (MPC). Although MPC presents high computational burden, it can easily handle

Manuscript received May 04, 2020; revised July 19, 2020 and August 14, 2020; accepted September 14, 2020. This work was made possible in part by the Fundamental Research Funds for the Central Universities under grant KG16034501, and in part by the Project funded by the State Key Laboratory of Safety Control and Simulation for Power Systems and Large Power Generation Equipment under grant SKLD20M05, China. (Corresponding Author: Yushan Liu)

X. Li and Y. Liu are with the School of Automation Science and Electrical Engineering, Beihang University, Beijing, 100083, China.

Y. Xue is with the Oak Ridge National Laboratory, Oak Ridge, TN 37831, USA.

multivariable case and system constraints and nonlinearities in a very intuitive way [22]-[27]. Instead of designing control loop and modulator for each operating mode separately as conventional methods, this controller regulates control objects along given reference through optimally choosing the switching state at each sampling sequence. Modulation and mode detection would be replaced by an optimization process through cost function. As a result, it can achieve automatic transition between modes inherently without extra design consideration when transferring between buck and boost modes. This largely simplifies the design and makes it easily implemented. As to the non-minimum phase behavior of the four-switch buck-boost converter, instead of regulating voltage directly, in the proposed controller, the control problem is formalized as a current regulation problem with variable frequency, allowing the controller optimizing switching states selection by a predictive controller. Moreover, contributing from the predictive current control design, the proposed controller could do switching optimization in every control cycle, which makes it with good transient performance. It also has capability to do current limit cycle by cycle per added current limit constrain in the cost function. By utilizing predicted current for overcurrent protection, the proposed controller would prevent overcurrent condition in advance of one sampling period, which helps improve system reliability. And the proposed controller is immune to line voltage variation due to the fact the switching optimization is based on sensed instantaneous input voltage.

Besides above mentioned features, the proposed method is also a potential solution for many applications, such as voltage regulation module, due to its easy regulation on many other performances that are critical in many system designs, such as over-current protection, under/overvoltage protection, light-load efficiency, line/load regulation and transient performance under variable input/load conditions. The proposed control shows the potential to easily implement those protection functions by integrating specific constrains into the cost function. It also exhibits fast transient response to both line and load variations. This controller also supports DCM operation. The switching states would be updated for DCM operation in a predetermined way with predicted current value. By utilizing the predicted current info to predetermine the DCM operation, it allows the system to take switching action one step ahead than conventional method based on sensed current information.

This paper proposes a novel control method for four-switch buck-boost converter, to eliminate the deadzone problem and achieve the seamless transfer between buck and boost operating conditions, while achieving other benefits on system performance. The organization of the paper is as follows: the operation of four-switch buck-boost converter and its deadzone issue are described in Section II; Section III presents the implementation detail of proposed control method; Section IV demonstrates simulation and experimental results; finally, in Section V, the conclusion of the work is provided.

II. OPERATION OF FOUR-SWITCH BUCK-BOOST CONVERTER

A. Operation Principle

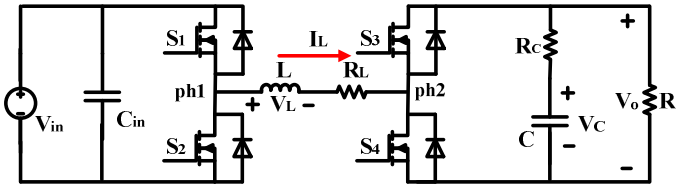

Fig. 1 Four-switch buck-boost converter.

Fig. 1 shows the non-inverting buck-boost converter, which contains four power switches, S1-S4, representing with corresponding body diode. The R_L represents the total series resistance of path, and R_C represents the total equivalent series resistance of output capacitor, where R_L includes inductor's resistance and any possible trace resistance in forward conduction path, such as on resistance of power switch.

The converter will operate as traditional synchronous boost if switch S1 keeps on and S2 keeps off, while S3 and S4 doing switching behavior. Similarly, it operates as synchronous buck if keeping S3 on and S4 off, while S1 and S2 switching. In condition when the input voltage, V_{in}, is closed to the output voltage, V_{out}, it is preferred for S1 and S3 to turned on and bypass the input directly with output side, preferred as bypass condition with small inductor current ripple and low loss.

Table I lists four possible active switching states in CCM, which have two switches turning on at the same time, while their complementary switches off to prevent shoot through.

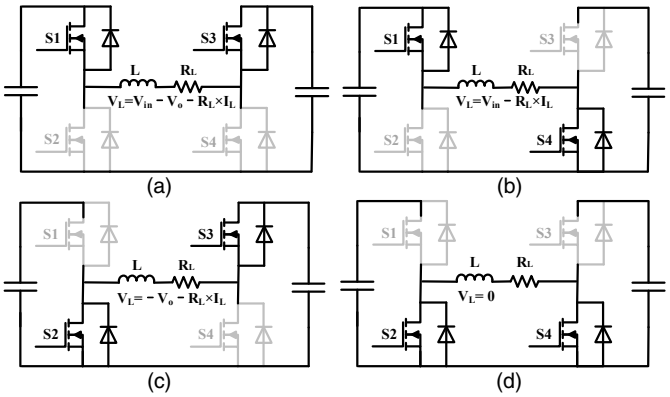

Fig. 2 Switching states of four-switch buck-boost converter in CCM. (a) State 1, (b) State 2, (c) State 3, (d) State 4.

TABLE I. SWITCHING CONFIGURATIONS AND PHASE NODE VOLTAGE IN CCM

States	S_1	S_2	S_3	S_4	*ph1*	*ph2*
State 1	1	0	1	0	Vin	Vo
State 2	1	0	0	1	Vin	0
State 3	0	1	1	0	0	Vo
State 4	0	1	0	1	0	0

TABLE II. TOTAL NUMBER OF CHANGING SWITCHES BETWEEN TWO SWITCHING STATES

Counts of switch changed, ***num_sw***	*State 1*	*State 2*	*State 3*
State 1	**0**	**2** (S_3, S_4)	**2** (S_1, S_2)
State 2	**2** (S_3, S_4)	**0**	**4** (S_1, S_2, S_3, S_4)
State 3	**2** (S_1, S_2)	**4** (S_1, S_2, S_3, S_4)	**0**

Fig. 2 shows the switching states corresponding to Table 1. State 1 in Fig. 2(a) represents the state during which S1 and S3 are turned on, S2 and S4 are turned off. This state could occur in buck mode, during which time the inductor gets charged energy or in boost mode, during which the inductor discharges the stored energy. State 2 in Fig. 2(b) is the state during which S1 and S4 are turned on, while S2 and S3 are turned off. This state occurs in boost mode during which more energy charges the inductor. State 3 in Fig. 2(c) is the state during which S2 and S3 are turned on, while S1 and S4 are turned off. This state occurs in buck mode when inductor discharges energy. State 4 in Fig. 2(d) represents the state during which S2 and S4 are turned on, while S1 and S3 are turned off. This state is utilized in neither buck nor boost mode. Thus, in order to simplify the optimization process and reduce calculating time of predictive process that is going to be introduced next, the switching states S1-S3 are mainly analyzed and selected as the effective switching states finally. For the same purpose, single-step prediction algorithm is examined mainly for small computation burden. Table II lists the total number of switches with changing state between two different switching states. The *num_sw* for example, from switching state 1 to state 2, there are two switches (S3 and S4) with the need to change its on/off status.

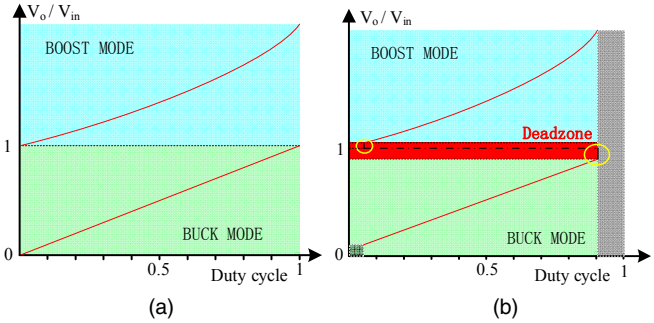

Fig. 3. Operation area of buck and boost modes. (a) Ideal case, and (b) real case.

B. Analysis on Buck-Boost Mode Transfer Issue

The steady-state input and output voltage relationship deriving from average model can be expressed as below, without considering the power loss and any possible parasitic parameters.

$$\frac{V_{out}}{V_{in}} = \begin{cases} D, & D \in [0,1] \\ \frac{1}{1-D}, & D \in [0,1] \end{cases} \quad (1)$$

Fig. 3(a) indicates the operation area of buck and boost mode in responding to their specific duty cycles. Ideally, by pulsating the buck phase or boost phase with a duty cycle from 0 to 1, the converter can operate in a full voltage window with seamless transfer between buck and boost mode, as indicated in Fig. 3(a). This is based on the assumption that the duty cycle ranges from 0 to 1, and the mode detection can be done in a reliable way to switch between buck and boost mode. However, this is not always the case. In power design, there is always min/max duty cycle limitation due to the gate driving delay, switching capacitances of power devices and possible bootstrap refresh requirements. Moreover, there is always dead-time consideration to prevent shoot through, which narrows the available duty cycle range, especially in high-frequency operation.

For analysis purpose, let's assume the min and max duty cycle is limited to 5% and 95% for both high-side and low-side switch of buck and boost phases. Then the workable region of buck and boost would be narrowed as indicated in Fig. 3(b). The region noted in red indicates the deadzone that is lost due to the "narrowed" duty cycle, while the zone noted in grey indicates other loss regions of original buck/boost working region that the circuit cannot work in any more.

The focus would be the deadzone, since it indicates that the converter cannot really regulates the V_o well if it is closed to V_{in}. It is related the maximum duty cycle available for buck phase and minimum duty cycle for boost phase. Now it is pretty clear that, by just using buck and boost modes with pulse width modulation, it is challengeable to do smooth transfer, due to the inherent deadzone resulting from the uncomplete duty cycle. The mode transfer issue would be more severe than this considering other non-ideal aspects, such as mode detection accuracy, loop performance of both buck and boost modes.

Even though there are some other methods trying to achieve so called seamless transfer between modes as mentioned in introduction, but most of them are just doing a way to allow buck phase and boost phase to operate simultaneously. This could reduce the deadzone largely, but also introducing other possible issues, such as high-switching loss during buck-boost mode, complexing the system design by adding an extra operating mode, and making the system more rely on accurate mode detection. Because of the parasitic parameters and tradeoffs between noise immunity and fast detection, it is hard to do mode detection in an accurate and fast way, which limits the system performance and increases the design cost. It would be good to have system method that does not rely on mode detection.

Moreover, in some operating conditions, the bypass mode is preferred, especially when the input voltage is very close to the output voltage. Most of existing control methods cannot realize this, since they would need the buck and boost to operate simultaneously in this condition by the way it is designed. This is not preferred in terms of ripple and efficiency.

All issues mentioned above would be solved easily by the proposed control scheme introduced in the following section.

III. Proposed MPC for Smooth Transition of Four-Switch Buck-Boost Converter

Fig. 4 shows the block diagram of the proposed control for this four-switch buck-boost converter. A cascaded structure with inner current loop and outer voltage loop is designed.

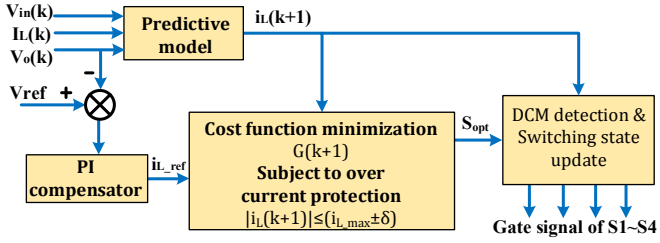

Fig. 4. Block diagram of proposed control strategy.

The inner loop is based on predictive current control, which regulates the inductor current with fast response speed. The outer loop is a voltage loop based on PI compensator, which takes the error between the output voltage of the converter and

its reference to calculate the required reference current of the inductor, i_{L_ref}, for the inner current predictive control.

The current reference i_{L_ref} is given by the outer output voltage loop with PI compensator, where the integration gain would contribute to reduce the accumulation error and decrease the regulation error in steady state. It follows the same PI control loop design rules. The inner current loop speeds up the transient, while the outer loop is mainly designed for regulation error reduction. For the inner predictive loop, firstly, system models containing main parasitic parameters are derived. Accordingly, current prediction can be conducted based on sensed info of power stage in each sampling interval. All selected active switching states are determined. The switching state that minimizes cost function g subject to the current limiter is selected and applied at the next sampling time k+1.

A. Predictive Model

The continuous time model of inductor current can be expressed as the following equation. Firstly, considering the state when S3 is on, and S4 is off. There is

$$L\frac{di_L(t)}{dt} = v_{in}(t)\cdot u_1(t) - i_L(t)\cdot R_L - v_o(t) \tag{2}$$

$$u_1(\mathrm{t}) = \begin{cases} 0; & S1 = off, S2 = on \\ 1; & S1 = on, S2 = off \end{cases} \tag{3}$$

And the output voltage can be derived based on inductor current, i_L, and output capacitor voltage, V_C, as the following equation.

$$v_o(t) = \frac{R[R_C i_L(t) + v_C(t)]}{R + R_C} \tag{4}$$

By merging (2) and (4), it can be derived that

$$L\frac{di_L(t)}{dt} = v_{in}(t)\cdot u_1(t) - R_L i_L(t) - \frac{R[R_C i_L(t) + v_C(t)]}{R + R_C} \tag{5}$$

Similarly, the capacitor voltage can be derived as

$$C\frac{dv_C(t)}{dt} = \frac{Ri_L(t)}{R + R_C} - \frac{v_C(t)}{R + R_C} \tag{6}$$

Secondly, considering the state when S3 is on, and S4 is off. There will be

$$L\frac{di_L(t)}{dt} = v_{in}(t)\cdot u_1(t) - R_L i_L(t) \tag{7}$$

Thus, combining (5) and (7), it can be derived that

$$L\frac{di_L(t)}{dt} = v_{in}(t)\cdot u_1(t) - R_L i_L(t) - \frac{R[i_L(t)R_C + v_C(t)]}{R + R_C}[1 - u_2(t)] \tag{8}$$

where

$$u_2(\mathrm{t}) = \begin{cases} 0; & S4 = off, S3 = on \\ 1; & S4 = on, S3 = off \end{cases} \tag{9}$$

Similarly, we can describe the capacitor voltage of two states in one equation written as

$$C\frac{dv_C(t)}{dt} = \frac{Ri_L(t)}{R + R_C}[1 - u_2(t)] - \frac{v_C(t)}{R + R_C} \tag{10}$$

And the output voltage can be represented by

$$v_o(t) = \frac{RR_C i_L(t)}{R + R_C}[1 - u_2(t)] + \frac{Rv_C(t)}{R + R_C} \tag{11}$$

Then according to the Euler method, the discrete-time predictive model of inductor current and capacitor voltage, and output voltage can be derived as in (12)-(14).

$$\begin{aligned} v_C(k+1) = {} & \left\{\frac{T_S\cdot R}{C(R + R_C)}[d_{aux} - u_2(k)] + 1\right\} i_L(k) \\ & - \frac{T_S}{C(R + R_C)} v_C(k) \end{aligned} \tag{13}$$

$$V_o(k) = \frac{R\cdot R_C}{R + R_C}[d_{aux} - u_2(k)] i_L(k) + \frac{R}{R + R_C} v_C(k) \tag{14}$$

where T_S is the sampling time. The discrete-time state-space model can be derived in a compact matrix form as

$$\begin{aligned} X(k+1) &= AX(k) + Bv \\ Y(k) &= CX(k) \end{aligned} \tag{15}$$

$$\begin{aligned} i_L(k+1) = {} & \left\{T_S\left[\frac{R\cdot R_C}{R + R_C}u_2(k) - \frac{R\cdot R_C}{L(R + R_C)}\cdot d_{aux} - \frac{R_L}{L}d_{aux}\right] + 1\right\} i_L(k) \\ & + T_S\left[\frac{R}{R + R_C}u_2(k) - \frac{R}{L(R + R_C)}\cdot d_{aux}\right] v_C(k) + \frac{T_S}{L}u_1(k)V_{in}(k) \end{aligned} \tag{12}$$

$$A = \begin{bmatrix} T_S\left[\frac{R\cdot R_C}{R + R_C}u_2(k) - \frac{R\cdot R_C}{L(R + R_C)}\cdot d_{aux} - \frac{R_L}{L}d_{aux}\right] + 1 & T_S\left[\frac{R}{R + R_C}u_2(k) - \frac{R}{L(R + R_C)}\cdot d_{aux}\right] \\ \frac{T_S\cdot R}{C(R + R_C)}[d_{aux} - u_2(k)] + 1 & \frac{T_S}{C(R + R_C)} \end{bmatrix}$$

$$B = \begin{bmatrix} \frac{T_S}{L}u_1(k) \\ 0 \end{bmatrix} \qquad C = \begin{bmatrix} \frac{R\cdot R_C}{R + R_C}[d_{aux} - u_2(k)] & \frac{R}{R + R_C} \end{bmatrix}$$

where $X(k) = [i_L(k)\ v_C(k)]^T$, $Y(k) = V_o$, $v = v_{in}(k)$, the coefficients, A, B, and C, are shown at the bottom of previous page. As [28], the d_{aux} in (12)-(14) is defined as

$$d_{aux} = \begin{cases} 1; & u_i(t) > 0, \text{or } u_i(t) = 0 \text{ and } i_L(t) > 0 \\ 0; & u_i(t) = 0 \text{ and } i_L(t) = 0 \end{cases} \tag{16}$$

where $i \in \{1, 2\}$.

So far, the discrete-time model and corresponding state-space model are derived that can be utilized for predictive control purpose.

B. Cost Function Definition

The characteristic of MPC allows to add linear and non-linear constraints to the controller, this is an advantage which is used in this paper to ensure the inductor current not exceed a certain maximum allowable value. This can be easily implemented by adding a corresponding weighting factor into

the cost function. The cost function of proposed predictive control is written as

$$g = \left|i_{L\_ref} - i_L(k+1)\right| + \lambda \times num\_sw + \lambda_{i\_limit} \quad (17)$$

The proposed MPC performs constrained multi-objective optimization. There are three items integrated in the cost function. The first one is the main one to track the inductor current reference by output voltage regulation purpose.

The second item is about switching frequency reduction. Due to the optimization principle, the switching frequency could be variable. Thus, in order to empower the average switching frequency reduction capability, this second item is added. In each sample interval, the changing switch count of every switching state corresponding to the last selected switching state would be counted, *num_sw*, according to Table II. Thus, the switching state with less switch change from last selected switching state would be easily selected because of this second item of cost function.

The third item is utilized to do overcurrent limit, where

$$\lambda_{i\_limit} = \begin{cases} 0, & i_L(k+1) < i_{max} \\ inf, & i_L(k+1) \geq i_{max} \end{cases} \quad (18)$$

It needs to be mentioned that, in conventional electrical system, overcurrent protection could be implemented with different response actions, such as shutdown, hiccup, current limit and foldback. Shutdown and hiccup can be implemented by state machine design following by a switch latch off for predetermined duration. While foldback and current limit action of overcurrent protection (OCP) normally needs loop support and is more challengeable for touch specs. In this design, it is targeted to have overcurrent protection with foldback and current limit cases. The foldback can be easily implemented by adjusting i_{max} in a predetermined way. This current-limit action without shutting down is needed in many applications, such as battery charging.

In this design, by adding this current limit related weighting factor into cost function, it would introduce three advantages: 1) It can implement a fast and smooth current limit function without shutting down part, but clamping the current to prevent it going higher; 2) it allows cycle by cycle over current protection; 3) by utilizing the predictive current value instead of just sensed current, it improves the robustness.

The switching frequency is considered as it determines the switching related power loss, which is a dominant loss in converter design. Switching loss, including commutation loss, gate driver loss and switch output cap related loss, engages in every switch turn on/off condition. Thus, switch transition count in every second needs to be taken care to largely indicate switching frequency info. The average switching frequency per semiconductor switch is defined as the average value of the switching frequencies in every second. As shown in Fig. 2, the total number of switching events, *num_sw*, required to alter from one state to others through possible switching paths is finite set, a look-up table (LUT) as Table II is constructed to store these information. The average switching frequency per cycle can be directly presented as

$$f_s = \frac{S_c(n_{k-t} : n_k)}{2} \quad (19)$$

where S_c represents the total number of switching events per second of four switches in four-switch buck-boost converter.

Fig. 5 represents the average switching frequency evaluation results in different conditions. In this evaluation case, the output voltage is fixed with 24V and running with 1us sampling time, then it varies input voltage in wide range from 9V to 39V, which covers buck, buck-boost and boost conditions. As shown in results, the system could work in bypass mode without switching ideally, assuming no need on boot-charge refresh, which benefits from the optimal control algorithm of proposed controller. Once the converter operates in buck and boost conditions in certain range, it is observed that the converter would operate in an average switching frequency closed to ½ sampling frequency in steady state. Fig 6 shows this relationship further, reflecting relationship between average switching frequency and sampling time, as well as weight factor λ used in (17). As expected, the higher sampling frequency and larger λ could result into a smaller average switching frequency.

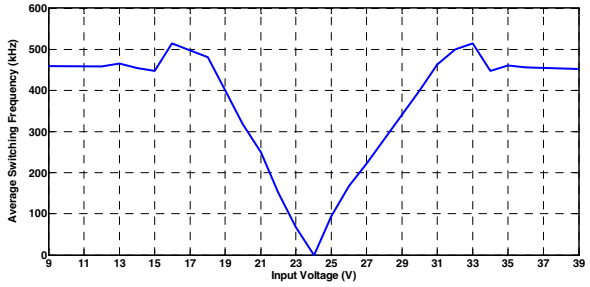

Fig. 5. Average switching frequency under different input condition.

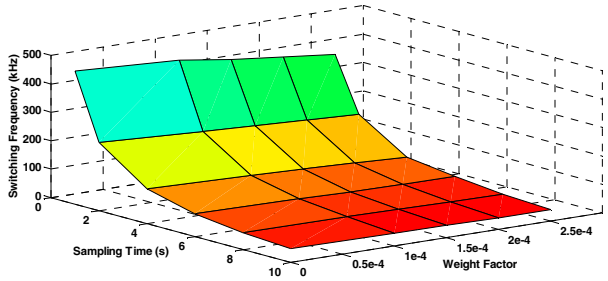

Fig. 6. Relationship between switching frequency and sampling time and weight factor.

C. Implementing Flowchat

The flowchart of proposed algorithm is illustrated in Fig.7. The λ_{i_limit} is updated based on (18) to prevent over current. In case of overcurrent event trigger, λ_{i_limit} is preferred to choose an infinite value theoretically. In real implementation, this would be an extremely large to make its weight over other factor in cost function. And when the tracking errors of output voltage are larger than the command threshold, λ=0, the controller gives more value and priorities to the current tracking in order to lower the tracking error. The switching event reduction objective is not functioning in this case. This situation may happen during the transient and improve the transient response of the controller. Mostly, an engineering trade-off needs to be identified to choose the right value for a certain application. Thus, the minimization of energy loss per switching event will be considered only in steady state in order to improve the dynamic performance of the system. Moreover,

this added weighting factor allows a way to dither the switching frequency and alter the system spectrum in some cases.

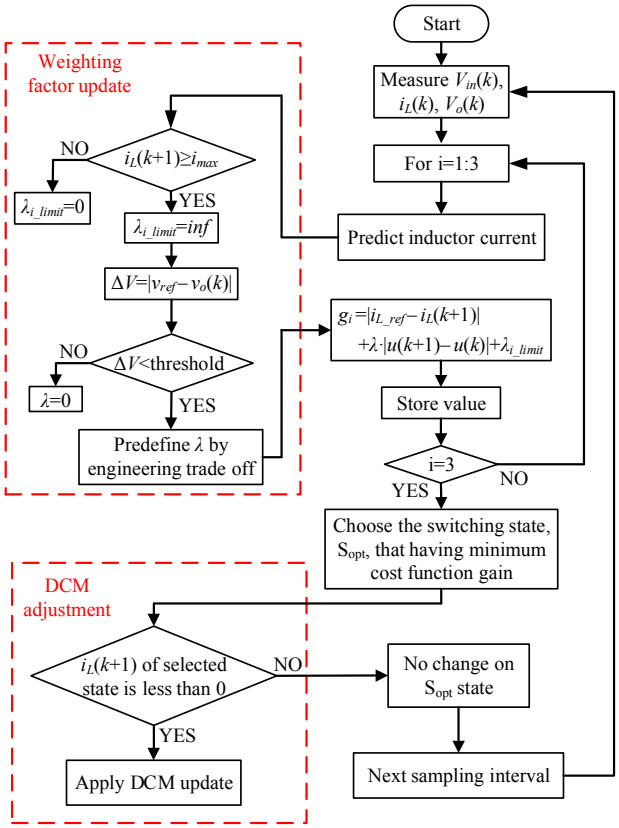

Fig. 7. Flowchart of proposed MPC-based control strategy.

It needs to be mentioned that, the proposed control does not need extra buck/boost mode detection. The need on separate loop design and modulator design for buck and boost modes in conventional methods is replaced by a shared optimization algorithm. Switching state would be optimized largely by considering the regulation purpose, regardless of V_{in}/V_{out} operating conditions. It could regulate the voltage in wide line and load variation ranges, indicating a good input voltage feedforward control effect, as a result of prediction modeling. This would largely ensure the mode seamless transition.

D. DCM Operation

As shown in the flowchart Fig. 7 of the proposed controller, the switching state would be optimized by tracking the reference current in each sampling interval. In normal conditions, the system operates in CCM depending on the sensed and predicted inductor current. Whenever the predicted inductor current of selected switching state for next sampling cycle is smaller than zero, the DCM adjustment action would be triggered, by turning off corresponding synchronous switch to adjust the inductor voltage second balance towards a stable and smooth direction.

The fundamental of DCM is to prevent negative inductor current causing extra power loss. In order to achieve that, there are two more switching states to be considered, as shown in Fig. 8. State 5 in Fig. 8 (a) would be preferred mostly when the converter operating in condition where input voltage is lower than output voltage, during which the inductor current freewheels through body diode of S3 while S3 switch is turned off to prevent negative current through inductor. State 6 in Fig. 8 (b) would be preferred mostly when the converter operating in condition where input voltage is higher than output voltage, during which the inductor current freewheels through body diode of S2 while S2 switch is turned off.

The switching states would be updated for DCM operation in a way as shown in Fig. 9 based on predicted current info. It is noted that this DCM adjustment would be designed to take action only when the predicted current corresponding to the selected optimal switching state is smaller than zero, which could guarantee the transient response of system. By utilizing the predictive current instead of sensing current, this gives the system more time window to detect and take action for DCM, which would be largely helpful for system designer, who suffers a lot from the zero crossing detection, trading off between noise immunity and system response time.

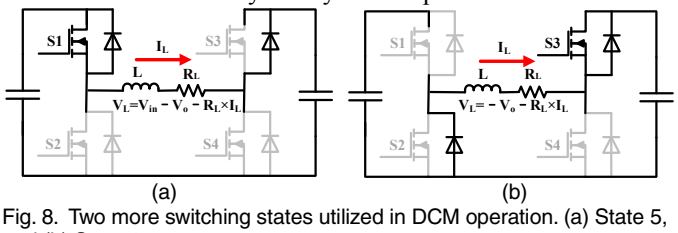

Fig. 8. Two more switching states utilized in DCM operation. (a) State 5, and (b) State 6.

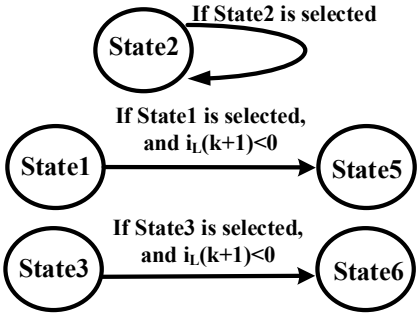

Fig. 9. State transfer for DCM operation.

E. Sensitive Analysis

In order to check the robustness of proposed method with parameter variations, sensitivity analysis on output voltage tracking error performance during steady state is conducted with variation on different critical parameters, as well as voltage transient performance checked.

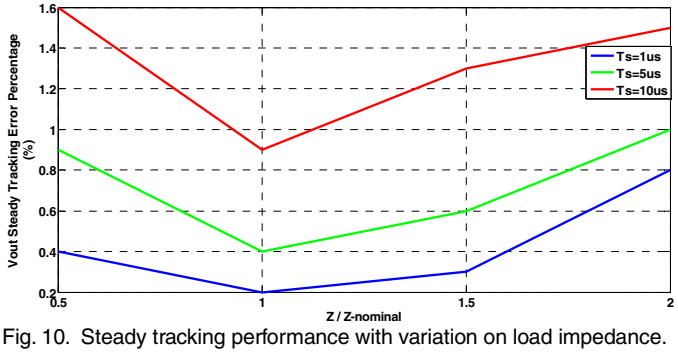

Fig. 10. Steady tracking performance with variation on load impedance.

Fig. 10 shows the output voltage tracking performance under uncertainty on load impedance with different sampling rates, 1us, 5us, and 10us sampling time respectively. As the

load impedance varies from 50% to 200%, the converter remains in the steady-state operating points with tracking error less than 2% in all evaluated conditions. As shown in results, the higher sampling rate, the smaller tracking error achieved. The presented results are in buck condition from 24V to 12V with nominated load impedance 5Ω and nominated L=50uH and C=600uH. The same conclusion works for other operating conditions and modes as checked.

In Fig. 11, the system parameters L and C vary from 80% to 120% of nominated values. It can be seen that the steady-state tracking error is always under 0.5% with sampling time of 1us. The tracking error enlarges as the sampling time gets larger, and it gets larger with more parameter variations from nominated value, but the tracking error is within 1.5% all the time, which indicates a good robustness to parameter variations.

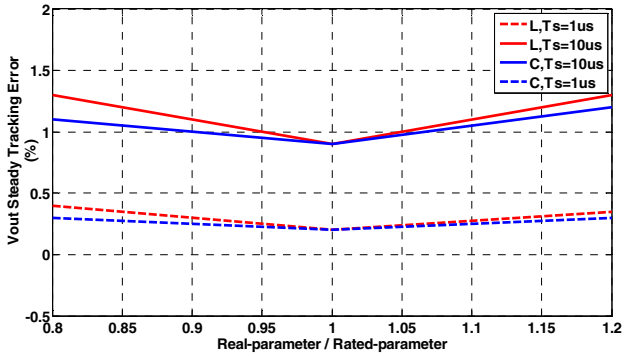

Fig. 11. Steady tracking performance with variation on L and C.

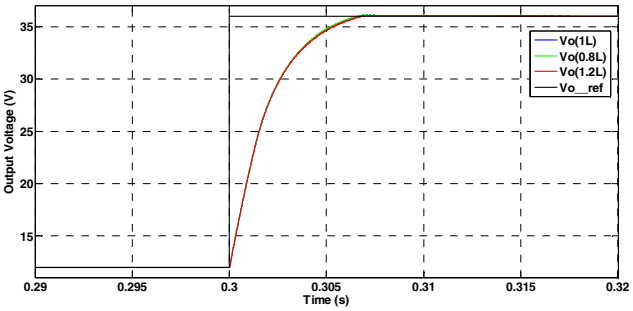

Fig. 12. Transient performance with variation on Inductance, L.

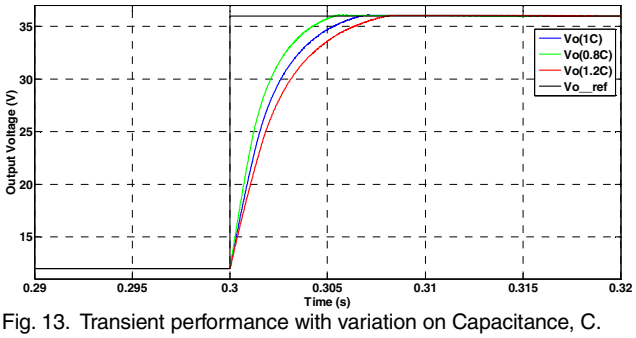

Fig. 13. Transient performance with variation on Capacitance, C.

Figs. 12 and 13 show the system transient performance with varied parameters (±20%) of inductance, L, and capacitance, C. As shown in Fig. 12, the performance in transient condition is almost same when there is an inductor parameter L ±20% mismatch. In Fig. 13, the output voltage transient gets slower than nominated case when the capacitor parameter C changes to 120% and gets faster when capacitor parameter changes to 80%. In all cases, the output voltage still tracks its reference value and reaches reference value quickly with little change on settling time as shown in results.

IV. Simulation Verification

TABLE III. System Parameters

Parameter	*Value*
Inductance, L	50 μH
Total series resistance of path, R_L	0.02 Ω
Output capacitance, C	600 μF
Equivalent series resistance of capacitor, R_C	0.05 Ω

The proposed control system of the four-switch buck-boost converter is evaluated in simulation through MATLAB, using system specifications listed in Table III as default case unless otherwise specified. In the simulation tests, both steady-state and dynamic performance of the output voltage regulation were evaluated, covering dynamic changes of reference output voltage, input line voltage, and load current.

The tuning of PI is compensated for the worst case in boost mode with full load to get higher dc gain and phase/gain margin [29]. The frequency response of the buck-boost converter is depicted in Fig. 14 with parameters in Table III and kp=0.056, ki=34.98, based on extended state averaging method [30].

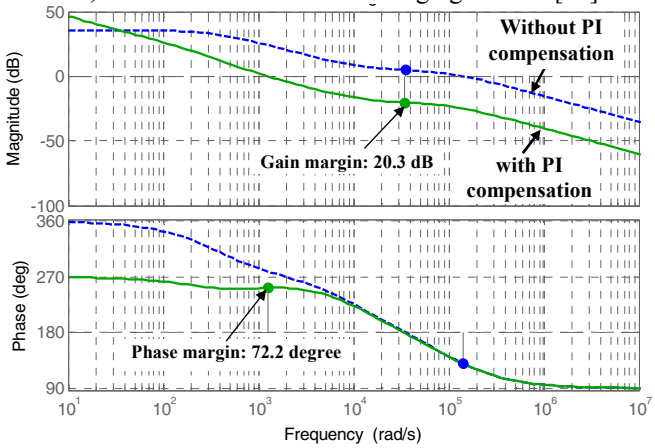

Fig. 14. Frequency response of the converter with PI compensation.

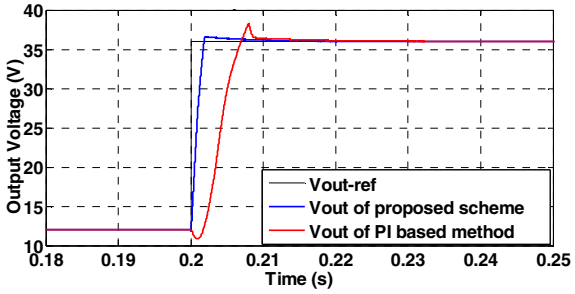

Fig. 15. Simulation results of output voltage step transient.

Fig. 15 shows the transient performance of system with reference voltage step change from 12V to 36V in both proposed method and PI based conventional method [1] with tuned parameters for transient and switching frequency closed to that of average switching frequency of proposed method. Sampling time of 1us is used for both methods. The input voltage is 24V with 5A constant current load connected at the output side of buck-boost converter. The system works in buck mode initially and then stays in boost mode eventually after going through a smooth transfer process. As shown in Fig. 15,

PI based method could go through a lagged transient and unregulated transient during mode transfer as a result of lagged mode transfer and loop switch. Comparatively, there is no obvious output voltage ripple and harsh response when it changes between buck and boost modes of proposed method.

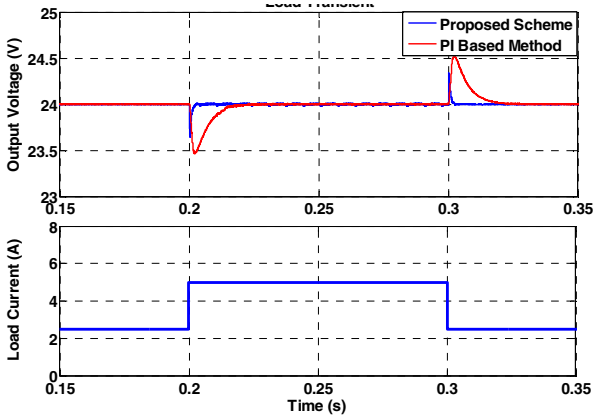

Fig. 16. Simulation results of step load current transient.

The four-switch buck-boost converter with the proposed control method is evaluated under fast-changing load and compared with conventional method. In this case, the reference output voltage is 24 V, and the 12 V input voltage is performed, i.e., the converter works in the boost mode. Then the load current changes from 2.5 A to 5 A with fastest available slew rate and changes back to 2.5 A. Fig. 16 shows simulation results of load transient. The proposed scheme can achieve better transient performance with smaller overshoot value and settling time. As shown in results, the output voltage keeps regulated stably, going through a smooth transient under load step changes. The observed ratios of overshoot and undershoot amplitudes of output voltage versus the stable value are within 2% under load transient.

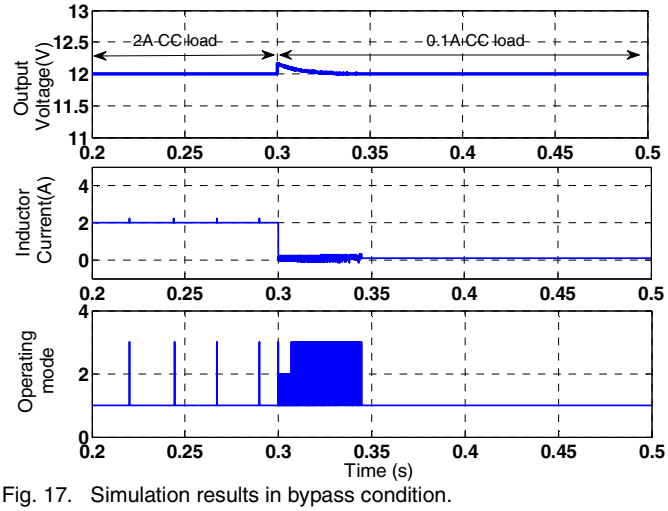

Fig. 17. Simulation results in bypass condition.

Fig. 17 shows the simulation results in bypass condition when the input voltage is equal to output voltage. In this simulated case, the input voltage and output reference value is same at 12V, and a constant-current load is applied with different values at different times, 2A before 0.3s and 0.1A after 0.3s respectively. As presented in Fig. 17, the converter can operate in bypass mode by choosing mode 1 (S1 and S3 on) for most of time, it is more obvious in light load condition when small power flows through power stage.

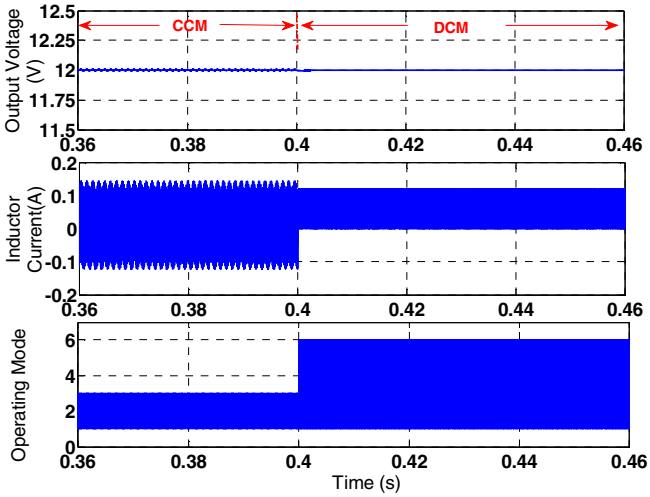

Fig. 18. Simulation results with both CCM and DCM operation.

Fig. 18 illustrates the DCM operation with light load, where a 0.01A constant current load is applied, and the DCM operation is allowed after 0.4 s. As shown in Fig. 18, the converter operates in CCM before 0.4 s with negative inductor current, and turns into DCM operation without any negative inductor current after time 0.4s, which reduced the inductor current ripple and conduction loss.

V. Experimental Verification

The proposed control system of four-switch buck-boost converter is evaluated in experiment, using system specifications listed in Table III as default case unless otherwise specified. The experimental setup is shown in Fig.19. Renesas RX600 DSC is utilized to implement control scheme with sampling time of 10us. Both the steady-state and dynamic performance of the output voltage regulation are evaluated.

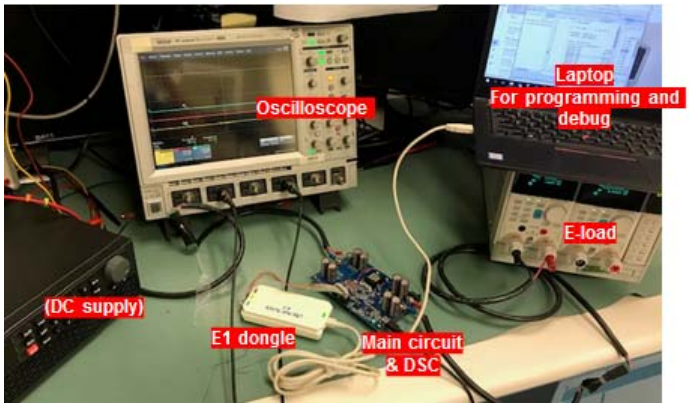

Fig. 19. Experimental setup.

Fig.20 shows the experimental results with output voltage step transient from 12 V to 36 V in case of 24V input voltage. There is a 5A constant current load connected at the output side of converter. As shown in result, the output voltage undergoes a smooth transfer process when it changes between buck and boost operation modes without obvious output voltage ripple. And the inductor current experiences fast transient without any large inrush current value. In addition, the output voltage tracks the reference value well with small tracking error in steady states, no matter which reference value. The observed tracking error is much less than 1% and small ripple performance with

less than 0.1% using a small output capacitance, which reduce the output capacitance needed in design.

Fig. 21 shows the case of input voltage step change from 12 V to 36 V while the output voltage reference stays at 24 V. Similarly, a 5A constant current source is connected as the load of converter. As shown in results, the output voltage returns to the 24 V through a fast regulation process after the input voltage change. The inductor current responses to the input voltage change at fast speed, without large inrush current. It can be seen that the system works in boost mode firstly and then transfers to buck mode smoothly after going through the buck-boost condition. As a result, the output voltage is under well regulation without effect of input voltage transient or operation mode transition.

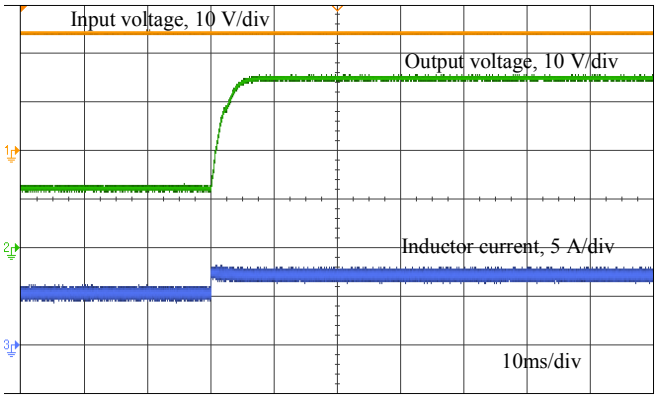

Fig. 20. Experimental results with output voltage change.

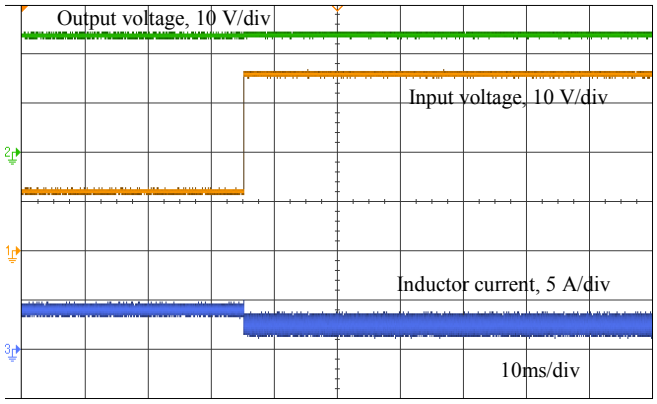

Fig. 21. Experimental results with input voltage change.

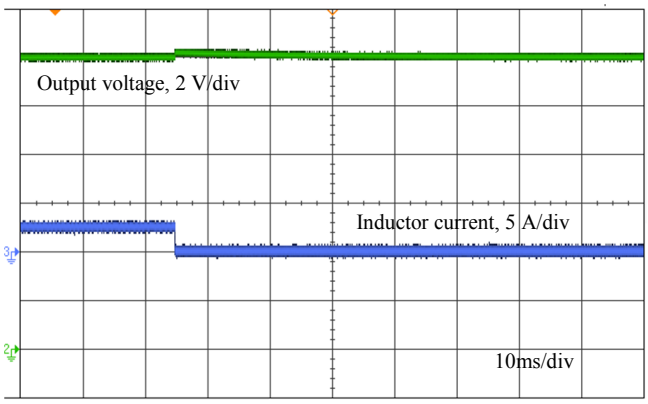

Fig. 22. Experimental results in bypass condition.

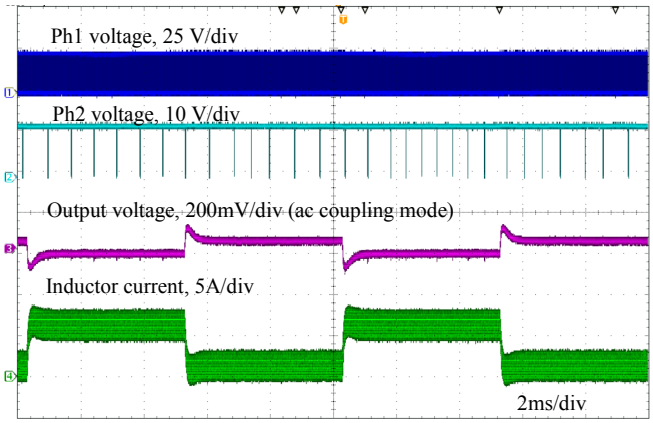

Fig. 23. Load transient with CCM.

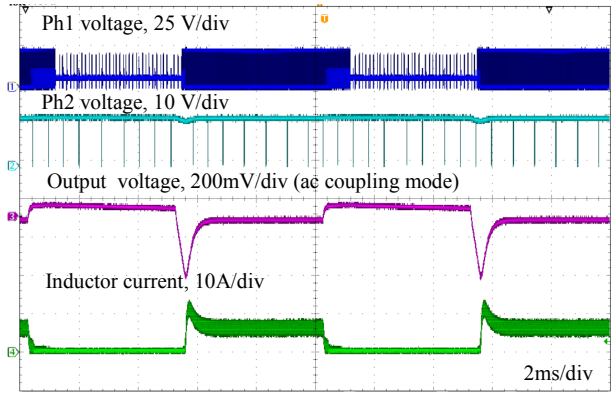

Fig. 24. Load transient with DCM enabled.

Fig.22 shows the results of 12V input voltage and 12V output voltage condition. In this evaluation case, the load step changes from 2A to 0.1A as simulation case. The output voltage was regulated stably and experiences a relatively smooth transient.

Fig.23 shows the load step transient performance in CCM mode from 10A to 0A in case of 24V input voltage and 12V output voltage. As shown in results, the output voltage keeps regulated stably, going through a smooth transient under load step changes. The observed ratios of overshoot and undershoot amplitudes of output voltage versus the stable value are within 2% under load transients. The inductor current changes sharply without large inrush value when the load current varies. However, at 0 load current case, the inductor current allows negative value as CCM feature. Fig. 24 shows the results in the same condition, but with DCM enabled. As indicated in results, DCM feature could disable negative current flowing through inductor through switch adjustment.

Fig.25 shows the measured efficiency of the converter operating in different conditions. As presented, The high input voltage results into larger switching loss at buck side, thus less efficiency, especially at light-load condition. At heavy-load condition, the efficiency difference is less due to the dominated conduction loss under this case. DCM function could improve efficiency at light load condition only. By choosing non-zero weight factor, the efficiency could be improved, with more obvious difference in light-load conditon as the results of reduced average switching frequency.

Table IV lists some key specifications for comparison between the proposed control method and conventional PI

based method [1]. In order for fair comparison, the conventional method control parameters are optimizied for transient and tracking performance firstly. The switching frequency was chosen to make it comparative to that of new method in tested condition without sacrifying transient much. By comparison with method 2 case 1, the proposed method could achieve higher peak efficiency in tested condition with similar tracking error performance. Comparing with method 2 case 2, it shows the proposed method could achieve faster transient and smaller tracking error by operating with switching frequency closed to conventional method. The added weight factor helps reduces switching frequency thus improving efficiency, but at the cost of lower tracking error and a little slower transient. Moreover, the proposed controller can achieve true bypass condition with smooth transfer between buck and boost modes.

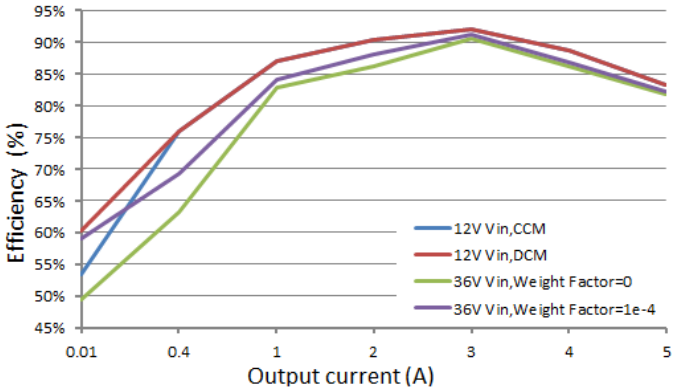

Fig. 25. Efficiency curve.

Table IV. Performance comparison summary

Parameter	Method 1	Method 2, Case 1	Method 2, Case 2	Method 2, Case 3
V_{out} Tracking error	0.8%	0.9%	0.4%	1.8%
Transient settling time	0.02 s	0.01 s	0.008 s	0.015 s
Average switching frequency	100kHz	49.9kHz	83.2kHz	43.5kHz
Peak efficiency	91.3%	93.5%	91.1%	92.6%
Smooth transfer between buck and boost	No	Yes	Yes	Yes

Note: Method 1 - Traditional multi-loop PI based power control method [1];
Method 2, case 1 - Proposed controller with weight factor as 0, Ts=10us;
Method 2, case 2 - Proposed controller with weight factor as 0, Ts=6us;
Method 2, case 3 - Proposed controller with weight factor as 1e-4, Ts=10us.

VI. Conclusion

In this paper, a MPC based control method was presented for the four-switch buck-boost converter, which is gaining popularity in both academy and industry. The proposed control method was proved to be effective to achieve smooth transfer without operating deadzone and reach good voltage regulation performance. The DCM operation was also allowed by the desgined controller. As the new method has inherent smooth transfer between modes without deadzone in modes, it shows potentials for many new applications, such as solar power optimizer and others mentioend in introduction. Simulation and experimental evalutions were conducted both steady and transient performances. Results demonstrated the effectiveness of proposed control for smooth transition between the buck and boost mode of the four-switch buck-boost converter, with fast response, accurate tracking and smooth transer capalbities.

References

[1] B. Sahu and G. A. Rincon-Mora, "A low voltage, dynamic, noninverting, synchronous buck-boost converter for portable applications," in *IEEE Transactions on Power Electronics*, vol. 19, no. 2, pp. 443-452, March 2004.

[2] C. Restrepo, J. Calvente, A. Cid-Pastor, A. E. Aroudi and R. Giral, "A Noninverting Buck–Boost DC–DC Switching Converter With High Efficiency and Wide Bandwidth," in *IEEE Transactions on Power Electronics*, vol. 26, no. 9, pp. 2490-2503, Sept. 2011.

[3] X. Hong, J. Wu and C. Wei, "98.1%-Efficiency Hysteretic-Current-Mode Noninverting Buck–Boost DC-DC Converter With Smooth Mode Transition," in *IEEE Transactions on Power Electronics*, vol. 32, no. 3, pp. 2008-2017, March 2017.

[4] X. Ren, X. Ruan, H. Qian, M. Li and Q. Chen, "Three-Mode Dual-Frequency Two-Edge Modulation Scheme for Four-Switch Buck–Boost Converter," in *IEEE Transactions on Power Electronics*, vol. 24, no. 2, pp. 499-509, Feb. 2009.

[5] X. Weng et al., "Comprehensive comparison and analysis of non-inverting buck boost and conventional buck boost converters," in *The Journal of Engineering*, vol. 2019, no. 16, pp. 3030-3034, 3 2019.

[6] C. Tsai, Y. Tsai and H. Liu, "A Stable Mode-Transition Technique for a Digitally Controlled Non-Inverting Buck–Boost DC–DC Converter," in *IEEE Transactions on Industrial Electronics*, vol. 62, no. 1, pp. 475-483, Jan. 2015.

[7] K. Xia, Z. Li, Y. Qin, Y. Yuan and Q. Yuan, "Minimising peak current in boundary conduction mode for the four-switch buck–boost DC/DC converter with soft switching," in *IET Power Electronics*, vol. 12, no. 4, pp. 944-954, 10 4 2019.

[8] J. Chen, P. Shen and Y. Hwang, "A High-Efficiency Positive Buck–Boost Converter With Mode-Select Circuit and Feed-Forward Techniques," in *IEEE Transactions on Power Electronics*, vol. 28, no. 9, pp. 4240-4247, Sept. 2013.

[9] K. Wu, H. Wu and C. Wei, "Analysis and Design of Mixed-Mode Operation for Noninverting Buck–Boost DC–DC Converters," in *IEEE Transactions on Circuits and Systems II: Express Briefs*, vol. 62, no. 12, pp. 1194-1198, Dec. 2015.

[10] Y. Lee, A. Khaligh and A. Emadi, "A Compensation Technique for Smooth Transitions in a Noninverting Buck–Boost Converter," in *IEEE Transactions on Power Electronics*, vol. 24, no. 4, pp. 1002-1015, April 2009.

[11] P. Huang, W. Wu and H. Ho"Hybrid Buck–Boost Feedforward and Reduced Average Inductor Current Techniques in Fast Line Transient and High-Efficiency Buck–Boost Converter," in *IEEE Transactions on Power Electronics*, vol. 25, no. 3, pp. 719-730, March 2010.

[12] C. Restrepo, T. Konjedic, J. Calvente, M. Milanovic and R. Giral, "Fast Transitions Between Current Control Loops of the Coupled-Inductor Buck–Boost DC–DC Switching Converter," in *IEEE Transactions on Power Electronics*, vol. 28, no. 8, pp. 3648-3652, Aug. 2013.

[13] C. Yao, X. Ruan, W. Cao and P. Chen, "A Two-Mode Control Scheme With Input Voltage Feed-Forward for the Two-Switch Buck-Boost DC–DC Converter," in *IEEE Transactions on Power Electronics*, vol. 29, no. 4, pp. 2037-2048, April 2014.

[14] K. Hariharan, S. Kapat and S. Mukhopadhyay, "Constant off-Time Digital Current-Mode Controlled Boost Converters With Enhanced Stability Boundary," in *IEEE Transactions on Power Electronics*, vol. 34, no. 10, pp. 10270-10281, Oct. 2019.

[15] Y. Tsai, Y. Tsai, C. Tsai and C. Tsai, "Digital Noninverting-Buck–Boost Converter With Enhanced Duty-Cycle-Overlap Control," in *IEEE Transactions on Circuits and Systems II: Express Briefs*, vol. 64, no. 1, pp. 41-45, Jan. 2017.

[16] D. C. Jones and R. W. Erickson, "A Nonlinear State Machine for Dead Zone Avoidance and Mitigation in a Synchronous Noninverting Buck–Boost Converter," in *IEEE Transactions on Power Electronics*, vol. 28, no. 1, pp. 467-480, Jan. 2013.

[17] M. Lin et al., "Authentic mode-toggled detector with fast transient response under wide load range buck-boost converter," *2013 IEEE International Symposium on Circuits and Systems (ISCAS)*, Beijing, 2013, pp. 2952-2955.

[18] C. Restrepo, T. Konjedic, J. Calvente and R. Giral, "Hysteretic Transition Method for Avoiding the Dead-Zone Effect and Subharmonics in a Noninverting Buck–Boost Converter," in *IEEE Transactions on Power Electronics*, vol. 30, no. 6, pp. 3418-3430, June 2015.

[19] C. Wei, C. Chen, K. Wu and I. Ko, "Design of an Average-Current-Mode Noninverting Buck–Boost DC–DC Converter With Reduced Switching and Conduction Losses," in *IEEE Transactions on Power Electronics*, vol. 27, no. 12, pp. 4934-4943, Dec. 2012.

[20] L. Jia, X. Sun, Z. Zheng, X. Ma and L. Dai, "Multimode Smooth Switching Strategy for Eliminating the Operational Dead Zone in Noninverting Buck–Boost Converter," in *IEEE Transactions on Power Electronics*, vol. 35, no. 3, pp. 3106-3113, March 2020.

[21] N. Zhang, G. Zhang and K. W. See, "Systematic Derivation of Dead-Zone Elimination Strategies for the Noninverting Synchronous Buck–Boost Converter," in *IEEE Transactions on Power Electronics*, vol. 33, no. 4, pp. 3497-3508, April 2018.

[22] S. Vazquez et al., "Model Predictive Control: A Review of Its Applications in Power Electronics," in *IEEE Industrial Electronics Magazine*, vol. 8, no. 1, pp. 16-31, March 2014.

[23] M. Novak, U. M. Nyman, T. Dragicevic and F. Blaabjerg, "Analytical Design and Performance Validation of Finite Set MPC Regulated Power Converters," in *IEEE Transactions on Industrial Electronics*, vol. 66, no. 3, pp. 2004-2014, March 2019.

[24] S. Kouro, P. Cortes, R. Vargas, U. Ammann and J. Rodriguez, "Model Predictive Control—A Simple and Powerful Method to Control Power Converters," in *IEEE Transactions on Industrial Electronics*, vol. 56, no. 6, pp. 1826-1838, June 2009.

[25] X. Li, H. Zhang, M. B. Shadmand and R. S. Balog, "Model Predictive Control of a Voltage-Source Inverter With Seamless Transition Between Islanded and Grid-Connected Operations," in *IEEE Transactions on Industrial Electronics*, vol. 64, no. 10, pp. 7906-7918, Oct. 2017.

[26] G. Zhou, J. Xu and B. Bao, "Comments on "Predictive Digital-Controlled Converter With Peak Current-Mode Control and Leading-Edge Modulation"," in *IEEE Transactions on Industrial Electronics*, vol. 59, no. 12, pp. 4851-4852, Dec. 2012.

[27] J. A. Rohten et al., "Model Predictive Control for Power Converters in a Distorted Three-Phase Power Supply," in *IEEE Transactions on Industrial Electronics*, vol. 63, no. 9, pp. 5838-5848, Sept. 2016.

[28] P. Karamanakos, T. Geyer and S. Manias, "Direct Voltage Control of DC–DC Boost Converters Using Enumeration-Based Model Predictive Control," in *IEEE Transactions on Power Electronics*, vol. 29, no. 2, pp. 968-978, Feb. 2014.

[29] P. Huang, W. Wu, H. Ho and K. Chen, "Hybrid Buck–Boost Feedforward and Reduced Average Inductor Current Techniques in Fast Line Transient and High-Efficiency Buck–Boost Converter," in *IEEE Transactions on Power Electronics*, vol. 25, no. 3, pp. 719-730, March 2010.

[30] T. Suntio, J. Lempinen, K. Hynynen and P. Silventoinen, "Analysis and small-signal modeling of self-oscillating converters with applied switching delay," APEC. *Seventeenth Annual IEEE Applied Power Electronics Conference and Exposition*, vol.1, pp. 395-401, Mar.2002.

Xiao Li (S'14–M'19) received the B.Sc. degree in Automation from Harbin Institute of Technology (HIT), China, in 2012, and the Ph.D. degree in Electrical Engineering from the Department of Electrical and Computer Engineering, Texas A&M University, College Station, TX, USA.

He is currently with School of Automation Science and Electrical Engineering, Beihang University, Beijing, China. His research interests include power electronics system integration, distributed generations, general power electronic circuit topologies, modeling and control, wide bandgap devices, etc.

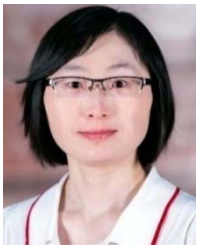

Yushan Liu (S'12–M'15–SM'19) received the B.Sc. degree in automation from Beijing Institute of Technology, Beijing, China, in 2008, and the Ph.D. degree in electrical engineering from the School of Electrical Engineering, Beijing Jiaotong University, Beijing, China, in 2014.

She was a Postdoctoral Fellow and an Assistant Research Scientist in the Department of Electrical and Computer Engineering, Texas A&M University at Qatar, Doha, Qatar, from 2014 to 2017. She is currently an Associate Professor in the School of Automation Science and Electrical Engineering, Beihang University, Beijing, China. She has published more than 80 journal and conference papers, one book, and one book chapter in the area of expertise. Her research interests include impedance source inverters, cascade multilevel converters, photovoltaic power integration, renewable energy systems, model predictive control, and smart transformers, etc.

Dr. Liu received the "Research Fellow Excellence Award" from Texas A&M University at Qatar, the "Excellent Doctoral Dissertations" Prize from Beijing Jiaotong University. She is an Associate Editor of the IEEE Transactions on Industrial Electronics and IEEE Open Journal of Industrial Electronics Society.

Yaosuo Xue (M'03–SM'12) received the B.Sc. degree in electrical engineering from East China Jiaotong University, Nanchang, China in 1991 and the M.Sc. degree in electrical engineering from the University of New Brunswick, Fredericton, Canada, in 2004.

From 1991 to 2000, he was an electrical engineer-in-charge in China Railway Design Corporation and led the traction power systems R&D of the first China's high-speed railway. In 2005-2006, he worked in Capstone Turbine Corporation as a Lead Power Electronics and Systems Engineer. During 2006 to 2008, he was a NSERC PGS-Doctor scholar at the University of New Brunswick. He was with Siemens Corporate Research from 2009 to 2015 and established Corporate Technology USA power electronics program. He is currently with Oak Ridge National Laboratory and his research interests include multilevel converters and smart inverter controls for renewable energy and utility applications.

He is an Associate Editor of the IEEE Transaction on Power Electronics and IEEE Journal of Emerging and Selected Topics in Power Electronics.